MRS Communications (2012), *2*, 101–105
© Materials Research Society, 2012
doi:10.1557/mrc.2012.17

MRS Communications

Research Letters

Direct correlation of *R*-line luminescence with rod-like defect evolution in ion-implanted and annealed silicon

S. Charnvanichborikarn, Lawrence Livermore National Laboratory, Livermore, California 94550; Department of Electronic Materials Engineering, Research School of Physics and Engineering, The Australian National University, Canberra, ACT 0200, Australia
J. Wong-Leung, Department of Electronic Materials Engineering, Research School of Physics and Engineering, The Australian National University, Canberra, ACT 0200, Australia; Centre for Advanced Microscopy, The Australian National University, Canberra, ACT 0200, Australia
C. Jagadish and **J.S. Williams,** Department of Electronic Materials Engineering, Research School of Physics and Engineering, The Australian National University, Canberra, ACT 0200, Australia

Address all correspondence to S. Charnvanichborikarn at **charnvanichb1@llnl.gov**

(Received 13 April 2012; accepted 27 July 2012)

Abstract

A quantitative correlation between *R*-line luminescence at around 1.37 μm and {311} defect nature, size and concentration has been undertaken in silicon, following keV Si-implantation and subsequent annealing using photoluminescence spectroscopy and plan-view transmission electron microscopy. The formation and evolution of the rod-like defects were found to be dependent on annealing time at a temperature of 700 °C, but there was no simple correlation found between the density and size of those defects and the *R*-line intensity. In particular, whereas the presence of {311} defects is essential for observing *R*-line luminescence, both very small {311} defects at short annealing times and fully developed {311} defects at long annealing times do not contribute to such luminescence. We provide possible explanations for this behavior and suggest that the local (strain) environment around defects, the dopant level and impurities in the silicon substrate may all play a role in determining *R*-line intensity.

The process of ion implantation in silicon produces damage and defects that usually undergo extensive diffusion, annihilation and agglomeration during heat treatment.[1,2] Some of the residual defects following annealing are optically active when excited by photons or electrons.[3,4] In such cases, the defects give rise to a defect state within the band gap of silicon that allows a direct sub-band gap transition and the emission of light. In particular, the interstitial-based defects (clusters and extended defects) in silicon can be optically active.[3] As the ion-implantation fluence and annealing temperature are raised, the residual defects evolve into interstitial defect clusters, rod-like defects (RLDs) and ultimately dislocations. The tri-Si-interstitial clusters, for example, are thought to be the origin of the *W*-line emission at 1218 nm.[5–7] The {311} RLDs are associated with *R*-line luminescence at 1372 nm,[3,8] while dislocations are associated with so-called D-bands at wavelengths above 1500 nm. The {311} RLDs have received much interest in the past decade mainly due to their ability to facilitate transient enhanced diffusion (TED) of boron, a common p-type dopant in silicon, when they dissociate to release a flux of Si-interstitials.[9] A comprehensive understanding of the TED process in the presence of {311} RLDs has become increasingly important as devices shrink to a sub-micron scale. Apart from this obvious technological importance, the structural and optical properties of {311} RLDs have also been of interest,[2,3] the latter for the possibility of enhancing light emission from silicon.[10] Previous studies have shown that the {311} defect is a chain of Si-interstitials with a {311} habit plane and extending along the ⟨110⟩ direction.[11] Their formation takes place after Si-implantation at sub-amorphizing fluences of the order of 10^{13} cm^{-2} and following annealing at a temperature between 600 and 850 °C.[12–14] In addition, Chou et al.[15] further reported that a small proportion of the RLDs (14%) had a {111} habit plane. Although, {311} RLDs have been proposed to be responsible for the *R*-line emission,[12,16] no quantitative correlation has yet been made between the *R*-line intensity and the nature (size and density) of RLDs and their environment. The current study addresses this issue.

In this work, photoluminescence (PL) and transmission electron microscopy (TEM) are used to monitor both the evolution and intensity of the *R*-line luminescence and to quantify the average concentration and nature (size) of implantation-induced RLDs as a function of annealing time. We find that there is no simple correlation between the *R*-line intensity and the RLD size or density, despite the fact that the presence of RLDs is essential for *R*-line luminescence. We suggest that the *R*-line intensity also appears to be sensitive to other effects such as local strain, the nature of disorder surrounding {311} defects or impurity effects.

Cz-grown boron-doped p-type (100) Si wafers with a resistivity of 5–25 Ω cm were irradiated at room temperature with 80 keV Si^- ions to a fluence of 5×10^{13} cm^{-2}, which produces

https://doi.org/10.1557/mrc.2012.17 Published online by Cambridge University Press

a large number of excess Si-interstitials and subsequent {311} defects beyond the ion projected range (~110 nm[17]) after annealing. We note that the chosen fluence is below a silicon amorphization threshold and was found to provide the optimum conditions for maximum *R*-line intensity for the ion energy used. The average scanned ion flux was kept constant at 3.45×10^{11} cm^{-2} s^{-1} to prevent unnecessary substrate heating. The implanted wafer was cut into several 3 mm diameter discs using a Gatan 601 ultrasonic cutter. A postimplantation anneal was then carried out for each sample in N_2 ambient with a fixed flow rate of ≈0.65 L/min from 10 to 90 min at 700 °C, where the sample was both inserted into and removed rapidly from the preheated furnace zone to promote rapid thermal ramping and cooling rates. Following annealing, the samples were mounted on a cryostat holder suitable for PL measurements and cooled to 13 K, where a 10 mW 532 nm laser was used to excite the luminescence. The PL spectra were dispersed by a SpectraPro-2500i triple grating monochromator equipped with a temperature-controlled InGaAs infrared photodetector. These same samples were used to prepare plan-view TEM specimens. The disc-shaped samples were mechanically thinned and dimpled from the backside down to about 10 μm at the center. Chemical etching was performed to perforate the samples, yielding large electron transparent regions. A Philips CM300 electron microscope operated at 300 kV was used to characterize all the TEM specimens. We examined regions of the foil that were thick enough to contain the RLD defect band entirely within the foil to ensure that the defects did not intersect the foil surfaces. All the TEM images were recorded under a weak-beam dark field (WBDF) condition using a *g*-*ng* diffraction arrangement, where $g = 022$ and $n = 3.2$. This imaging condition was used to survey the defect density but detailed Burgers vector determination of the RLDs was not carried out within the scope of this work. The inclination of the defect lines with respect to the TEM foil (as observed by an oscillating (dotted) contrast)[18] is also taken into account when determining the size of the defect.

Figure 1 shows the PL spectra measured at 13 K from the Si-implanted samples isothermally annealed at 700 °C for different time periods from 10 to 90 min. The signal from silicon band-edge luminescence Si_{TO} at 1130 nm is observed in all the spectra and becomes brighter with increasing annealing time, as a result of a progressive reduction in the overall implantation-induced disorder. Annealing for 10 min results in a small but broad peak centered around 1350 nm, and a larger and broader feature beyond 1400 nm. Unlike the Si_{TO}, the *R*-line luminescence is observed only after annealing from 20 to 60 min. Indeed, the *R*-line is maximized in intensity by 40 min and disappears completely by 90 min. At first sight, the loss of *R*-line intensity after 90-min annealing is in disagreement with a previous study, where a strong *R*-line was observed after annealing at 700 °C for at least an hour.[19] However, the implantation regime used in this previous study (1.2 MeV Si to a fluence of 10^{13} cm^{-2}) is expected to initiate a different defect evolution pathway during annealing from that in our study.

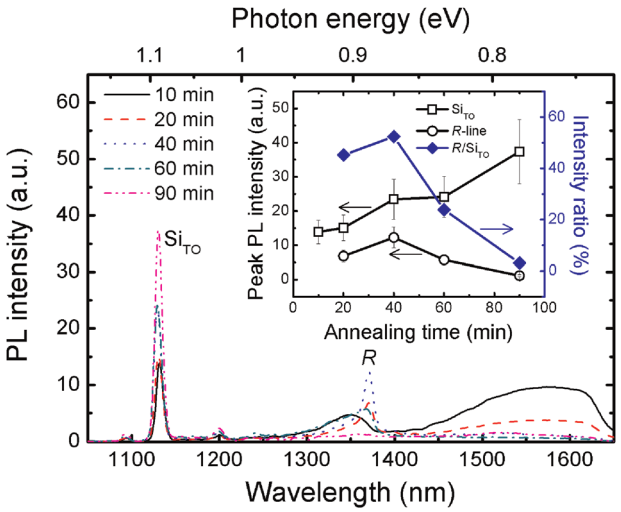


Figure 1. PL spectra for silicon samples implanted with 80 keV Si ions to a fluence of 5 × 1013 cm^{-2} and a subsequent anneal at 700 °C for various times. The inset displays intensities of a silicon peak (open squares) and the R-line (open circles) as a function of annealing time. The intensity ratio of the R-line to silicon peak (solid diamonds) is plotted in the right ordinate.

We note after 60-min annealing that the *R*-line peak is not only lower in intensity but also slightly shifted to shorter wavelength. It is also noteworthy that a longer wavelength broad luminescence band (from 1425 to 1650 nm) is observed in most of the cases, and is particularly strong at annealing times ≤20 min. Thus, it is tempting to speculate that this broad feature may arise from either small interstitial clusters[20] or strained regions[21] that have not fully evolved into extended defects, a fact that is clarified later by TEM.

In order to interpret the PL spectra, it is important to treat the effect of implantation damage carefully. The process of ion-implantation usually introduces lattice damage that contributes to the formation of non-radiative recombination centers, leading to an overall loss of luminescence intensity. Harding et al.[22] have suggested that the effect of radiation damage may be gauged by examining the intensity of the relevant peak (*R*-line) relative to the silicon (Si_{TO}) peak. The inset of Fig. 1 plots the PL peak intensities of the *R*-line (open circles) and Si_{TO} (open squares) peak against the annealing time, while the intensity ratio of the *R*-line to Si_{TO} for each annealing time is shown with respect to the right-hand axis. Clearly, the *R*-line intensity drops after 40 min, whereas the Si_{TO} increases as the implantation damage is removed.

Figure 2 shows representative plan-view TEM images of the corresponding samples. The RLDs exist in all samples; however, they are not well formed and are very dilute in the 10-min annealed sample [Fig. 2(a)]. Indeed, most of the defects observed after 10-min annealing are nanometer-sized clusters, which may be regarded as possible precursors of the RLDs. The inset of Fig. 2(a) shows a close-up image of embryonic RLDs and clearly indicates a preferential line orientation in

https://doi.org/10.1557/mrc.2012.17 Published online by Cambridge University Press

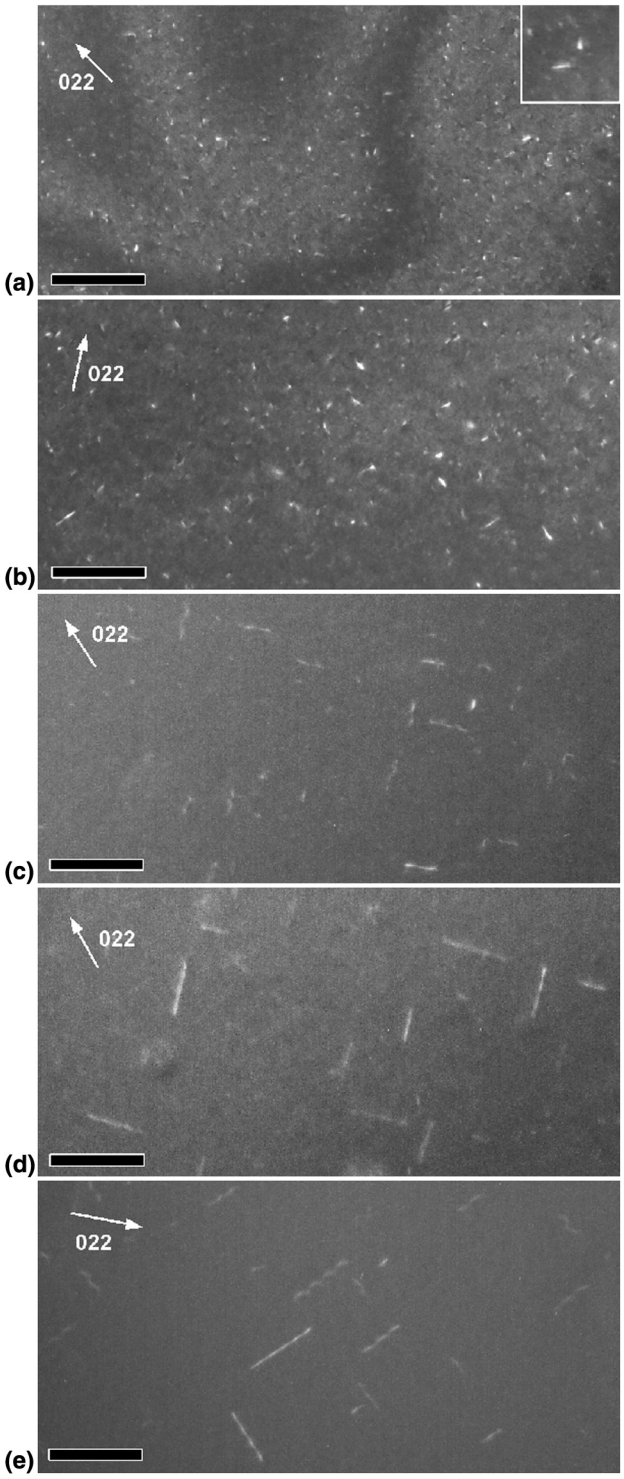


Figure 2. WBDF micrographs illustrating in plan-view RLDs formed in silicon by 80 keV Si-ion implantation and subsequent 700 °C annealing for (a) 10 min, (b) 20 min, (c) 40 min, (d) 60 min and (e) 90 min. The scale bars represent 100 nm.

spite of its short dimension. The other samples annealed from 20 to 90 min are illustrated in Figs. 2(b)–2(e). In fact, the RLDs can clearly be found to elongate in ⟨110⟩ directions after annealing for 40 min. The size distributions of the RLDs are compared for the various annealing times in Fig. 3.

As shown in Fig. 3, the defect distribution changes significantly with increasing annealing time. These interstitial-based RLDs gradually grow (at a non-linear rate) with time up to 60 min but their average length ($\bar{X}$) remains virtually constant on further annealing, consistent with a previous finding.[23] The RLD concentration (σ), on the other hand, decreases abruptly during the 20- to 40-min period but more slowly upon prolonged annealing. This observation suggests a growth of the RLDs, and the liberation of interstitials during the annealing.[24,25] Assuming that 1 nm of an RLD contains 20 interstitials,[24,26] it is possible to estimate the number of Si-interstitials (n_i) involved in RLDs from the distributions, which is given in each case in Fig. 3. The loss of interstitials from the RLDs during growth and dissolution is about 30% between 20 and 40 min and becomes less significant for further annealing up to 90 min.

Previous work has correlated the *R*-line luminescence to the presence of the {311} defects.[12] However, the present study has provided a quantitative correlation that illustrates that the presence of {311} defects alone is not sufficient to guarantee *R*-line luminescence. In our case, where the majority of defects appear to be ill-defined interstitial clusters in the 10-min annealed samples, the lack of *R*-line luminescence may be a result of the small size of the {311} defects. Indeed, Schmidt et al.[8] have argued that *R*-line luminescence is not observed in samples containing very short {311} defects of size $\lesssim$5 nm. Thus, a more complex explanation is required to explain the disappearance of the *R*-line (and the evolution of the luminescence spectrum) for the 90-min anneal since there is little change in the size and density of the RLDs between the 60- and 90-min-annealed cases. Furthermore, the intensities of the *R*-line luminescence in the 20- and 40-min-annealed samples are comparable (within a factor of 2), although the distribution profiles of the RLDs are widely different. Specifically, the sample annealed for 20 min contains a high concentration of short RLDs, while those in the sample annealed for 40 min are undoubtedly fewer and much longer (see Fig. 3). This suggests that RLDs of different sizes may contribute unequally to the *R*-line luminescence.

Based on the above results, an explanation of *R*-line luminescence based solely on an optimum RLD size is questionable. Furthermore, the estimated total number of Si-interstitials that are trapped in RLDs in 60- and 90-min anneal cases is similar, hence the *R*-line intensity does not scale with the number of Si interstitials. Let us now explore some other possibilities to explain our results such as strain-stimulated luminescence from {311} defects and the role of competing quenching mechanisms that can decrease the *R*-line intensity.

Firstly, local strain surrounding defects has previously been proposed as a contributing factor in radiative recombination associated with RLDs that gives rise to the *R*-line.[16] Although our TEM analysis of strain fields around the defects could not be quantified, it remains possible that the strain

https://doi.org/10.1557/mrc.2012.17 Published online by Cambridge University Press

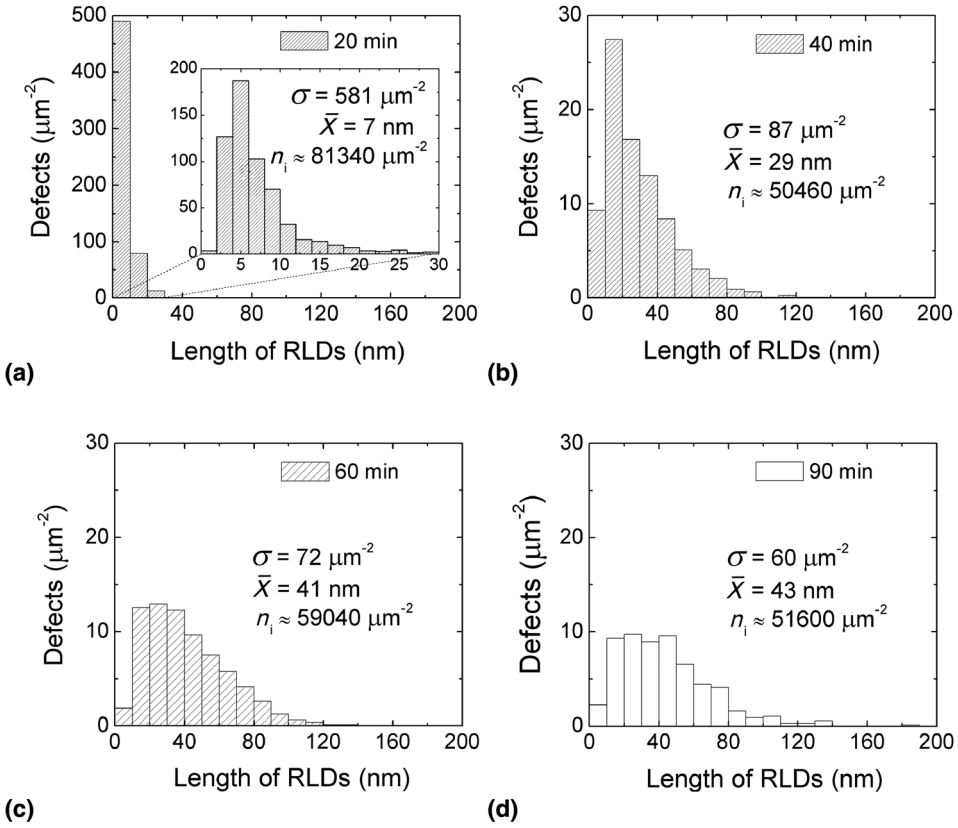


Figure 3. Statistical collection illustrating the size and density of the RLDs distributed after annealing at 700 °C for (a) 20 min, (b) 40 min, (c) 60 min and (d) 90 min. The inset of (a) shows a distribution of RLD after 20 min annealing in a refined scale.

surrounding {311} defects, and its relaxation at longer annealing times can explain our results. Secondly, as shown in Table I, the concentration of {311} defect sizes <5 nm is highest after 20-min annealing and decreases abruptly with increasing annealing time. On the other hand, the concentration of larger {311} defects (>5 nm) increases with annealing time up to 40 min and then decreases, which follows the trend of the R/Si_{TO} intensity ratio but the latter decreases well over an order of magnitude more rapidly. This observed relationship is in agreement with the previous finding that the small size {311} defects (≤5 nm), of which surrounding strain may not have fully developed, do not give rise to the *R*-line.[8] However, the intensity ratio of the *R*-line decreases at a much faster rate than the evaporation of the large RLDs (>5 nm). It is possible that the prolonged anneal may lead to a state where the surrounding strain is reduced as the RLDs further develop and is not sufficient to assist exciton recombination at the defect sites. Finally, processes competing with luminescence from {311} defects such as other non-radiative recombination centers associated with irradiation damage,[22] quenching by dopant effects and trapping of impurities at defects[27,28] may play an important role, especially at long annealing times. For example, gettering of (metal) impurities to dislocations has previously been suggested as a possible cause for observed changes in band-edge luminescence.[29,30]

Table 1. Defect density and R-line luminescence intensity for different annealing times.

Annealing time (min)	Defect density (μm^{-2})		R/Si_{TO} (%)
	≤5 nm	>5 nm	
10	–	–	–
20	372	523	95.2
40	4	678	122.2
60	0	573	49.5
90	0	448	2.8

In summary, we have conducted experiments to quantitatively investigate the link between *R*-line luminescence and physical properties of the corresponding RLDs formed by Si-implantation and thermal annealing. Our observations suggest that the relationship between the RLD size and density and *R*-line luminescence intensity is complicated, whereby very small RLDs under 5 nm contribute minimally to the *R*-line intensity. Other factors such as the local strain

https://doi.org/10.1557/mrc.2012.17 Published online by Cambridge University Press

surrounding the defect regions and residual damage, dopant effects or impurities could potentially influence detection of the *R*-line at longer annealing times.

Acknowledgments

One of the authors (S.C.) thanks Bianca Haberl for assistance in TEM sample preparation. This work was funded by the Australian Research Council. This work was performed under the auspices of the U.S. DOE by LLNL under Contract DE-AC52-07NA27344.

References

1. E. Chason, S.T. Picraux, J.M. Poate, J.O. Borland, M.I. Current, T. Diaz de la Rubia, D.J. Eaglesham, O.W. Holland, M.E. Law, C.W. Magee, J.W. Mayer, J. Melngailis, and A.F. Tasch: Ion beams in silicon processing and characterization. *J. Appl. Phys.* **81**, 6513 (1997).
2. S. Libertino and A. La Magna: Damage formation and evolution in ion-implanted crystalline Si, in *Materials Science with Ion Beams*, Topics in Applied Physics Vol. **116**, edited by H. Bernas (Springer-Verlag, Berlin, 2010), pp. 147–212.
3. G. Davies: The optical properties of luminescence centres in silicon. *Phys. Rep.* **176**, 83 (1989).
4. S. Charnvanichborikarn: Defect-Mediated Nanostructures and Luminescence Centres in Silicon. Ph.D. Thesis, The Australian National University (2011).
5. G. Davies, E.C. Lightowlers, and Z.E. Ciechanowska: The 1018 meV (W or I_1) vibronic band in silicon. *J. Phys. C* **20**, 191 (1987).
6. B.J. Coomer, J.P. Goss, R. Jones, S. Öberg, and P.R. Briddon: Interstitial aggregates and a new model for the I_1/W optical centre in silicon. *Physica B* **273–274**, 505 (1999).
7. P.K. Giri: Photoluminescence signature of silicon interstitial cluster evolution from compact to extended structures in ion-implanted silicon. *Semicond. Sci. Technol.* **20**, 638 (2005).
8. D.C. Schmidt, B.G. Svensson, M. Seibt, C. Jagadish, and G. Davies: Photoluminescence, deep level transient spectroscopy and transmission electron microscopy measurements on MeV self-ion implanted and annealed *n*-type silicon. *J. Appl. Phys.* **88**, 2309 (2000).
9. D.J. Eaglesham, P.A. Stolk, H.-J. Gossmann, and J.M. Poate: Implantation and transient B diffusion in Si: the source of the interstitials. *Appl. Phys. Lett.* **65**, 2305 (1994).
10. Y. Yasutake, J. Igarashi, N. Tana-ami, and S. Fukatsu: An electric-field-active 1377-nm narrow-line Si light-emitting diode at 150 K. *Opt. Express* **17**, 16739 (2009).
11. M.D. Matthews and S.J. Ashby: The dynamic observation of the formation of defects in silicon under electron and proton irradiation. *Philos. Mag.* **27**, 1313 (1973).
12. S. Coffa, S. Libertino, and C. Spinella: Transition from small interstitial clusters to extended {311} defects in ion-implanted Si. *Appl. Phys. Lett.* **76**, 321 (2000).
13. P.K. Giri, S. Coffa, and E. Rimini: Evidence for small interstitial clusters as the origin of photoluminescence *W* band in ion-implanted silicon. *Appl. Phys. Lett.* **78**, 291 (2001).
14. G. Davies, R. Harding, T. Jin, A. Mainwood, and J. Leung-Wong: Optical studies of ion-implantation centres in silicon. *Nucl. Instrum. Methods Phys. Res. B* **186**, 1 (2001).
15. C.T. Chou, D.J.H. Cockayne, J. Zou, P. Kringhøj, and C. Jagadish: {111} defects in 1-MeV-silicon-ion-implanted silicon. *Phys. Rev. B* **52**, 17223 (1995).
16. E.C. Lightowlers, L. Jeyanathan, A.N. Safonov, V. Higgs, and G. Davies: Luminescence from rod-like defects and hydrogen related centres in silicon. *Mater. Sci. Eng., B* **24**, 144 (1994).
17. J.P. Biersack and L.G. Haggmark: A Monte Carlo computer program for the transport of energetic ions in amorphous targets. *Nucl. Instrum. Methods* **174**, 257 (1980).
18. J. Wong-Leung, S. Fatima, C. Jagadish, J.D. Fitz Gerald, C.T. Chou, J. Zou, and D.J.H. Cockayne: Transmission electron microscopy characterization of secondary defects created by MeV Si, Ge, and Sn implantation in silicon. *J. Appl. Phys.* **88**, 1312 (2000).
19. S. Libertino, S. Coffa, C. Spinella, A. La Magna, and V. Privitera: Point defect diffusion and clustering in ion implanted c-Si. *Nucl. Instrum. Methods Phys. Res. B* **178**, 25 (2001).
20. N.E.B. Cowern, G. Mannino, P.A. Stolk, F. Roozeboom, H.G.A. Huizing, J.G.M. van Berkum, F. Cristiano, A. Claverie, and M. Jaraíz: Energetics of self-interstitial clusters in Si. *Phys. Rev. Lett.* **82**, 4460 (1999).
21. H. Weman, B. Monemar, G.S. Oehrlein, and S.J. Jeng: Strain-induced quantum confinement of carriers due to extended defects in silicon. *Phys. Rev. B* **42**, 3109 (1990).
22. R.E. Harding, G. Davies, S. Hayama, P.G. Coleman, C.P. Burrows, and J. Wong-Leung: Photoluminescence response of ion-implanted silicon. *Appl. Phys. Lett.* **89**, 181917 (2006).
23. K. Moller, K.S. Jones, and M.E. Law: Cross-sectional transmission electron microscopy analysis of {311} defects from Si implantation into silicon. *Appl. Phys. Lett.* **72**, 2547 (1998).
24. P.A. Stolk, H.-J. Gossmann, D.J. Eaglesham, D.C. Jacobson, C.S. Rafferty, G.H. Gilmer, M. Jaraíz, J.M. Poate, H.S. Luftman, and T.E. Haynes: Physical mechanisms of transient enhanced dopant diffusion in ion-implanted silicon. *J. Appl. Phys.* **81**, 6031 (1997).
25. G.Z. Pan and K.N. Tu: Transmission electron microscopy on {113} rodlike defects and {111} dislocation loops in silicon-implanted silicon. *J. Appl. Phys.* **82**, 601 (1997).
26. S. Takeda: An atomic model of electron-irradiation-induced defects on {113} in Si. *Jpn. J. Appl. Phys.* **30**, L639 (1991).
27. T.E. Haynes, D.J. Eaglesham, P.A. Stolk, H.-J. Gossmann, D.C. Jacobson, and J.M. Poate: Interactions of ion-implantation-induced interstitials with boron at high concentrations in silicon. *Appl. Phys. Lett.* **69**, 1376 (1996).
28. R. Brindos, P. Keys, K.S. Jones, and M.E. Law: Effect of arsenic doping on {311} defect dissolution in silicon. *Appl. Phys. Lett.* **75**, 229 (1999).
29. V. Higgs, E.C. Lightowlers, C.E. Norman, and P. Kightley: Characterisation of dislocations in the presence of transition metal contamination. *Mater. Sci. Forum* **83–87**, 1309 (1992).
30. A.N. Tereshchenko, E.A. Steinman, and A.A. Mazilkin: Effect of copper on dislocation luminescence centers in silicon. *Phys. Solid State* **53**, 369 (2011).

https://doi.org/10.1557/mrc.2012.17 Published online by Cambridge University Press